

Interaction of 0.53 μm laser pulse with millimeter-scale plasmas generated with gas-bag target

Jian Zheng^{1,a}, Zhi-chao Li^{1,2}, Xiao-hua Jiang², Zhe-bin Wang², Bin Zhao¹, Guang-yue Hu¹, Qiang Yin², Feng Wang², Xiao-shi Peng², Fang-hua Zhu², San-wei Li², Zheng Yuan², Yong-gang Liu², Li Chen², Peng Yuan¹, Liang Guo^{1,2}, Shen-ye Liu² and Yong-kun Ding²

¹ CAS Key Laboratory of Basic Plasma Physics and Department of Modern Physics, University of Science and Technology of China, Hefei, Anhui 230026, PR China

² Research Center of Laser Fusion, China Academy of Engineering Physics, Mianyang, Sichuan 621900, PR China

Abstract. Reported are the interactions of 0.53 μm laser pulse with millimeter-scale plasmas that are produced with gas-bag target irradiated with 0.35 μm laser pulses. The generated plasmas are characterized with collective Thomson scattering and space- and time-resolved X-ray images. The density of the plasmas is about $0.1 n_c$ corresponding to the 0.53 μm laser beam, and the temperature is about 0.64 keV with a filling gas of C_5H_{12} . The interaction laser beam can output 1.0 kJ energy within the duration of 1 ns at the wavelength of 0.53 μm , leading to a nominal intensity less than $1.5 \times 10^{15} \text{ W/cm}^2$. The reflectivity of stimulated Brillouin scattering (SBS) and stimulated Raman scattering (SRS) is measured with a full aperture backscatter system. The experimental results show that the reflectivity of SBS is less than 5% and that of SRS is less than 1%. It is a positive result with respect to using 0.53 μm lasers as drivers for laser fusion.

1. INTRODUCTION

Blue laser beams with a wavelength of 0.35 μm have been extensively used for the experimental research of inertial confinement fusion for more than two decades [1], and are now employed to achieve ignition [2] because of their higher inverse bremsstrahlung absorption efficiency and lower level of laser-plasma instabilities (LPIs) in comparison with those with longer wavelength [3]. However, the price of ultraviolet beams is high: rather low frequency conversion efficiency and serious damage problem for the optic components in the final optic assembly, that limit the maximum energy output capability. Due to the higher frequency conversion efficiency and the higher damage threshold on optics, the beam energy of green laser with a wavelength of 0.53 μm can exceed the value by the factor of 1.5 in comparison with that of blue laser. Therefore, there could be a larger target design space to achieve ignition with green laser beams [4]. One of the key issues of the green lasers for ICF experiments is the level of LPIs because the growth rate of LPIs is usually proportional to $I\lambda^2$, where I is the laser intensity and λ is the laser wavelength [3]. If the LPIs driven by green laser beams could remain at an acceptable level, high-gain capsule may be ignited with green lasers. Up to now, there are only a few articles addressing this subject [5–7].

^ae-mail: jzheng@ustc.edu.cn

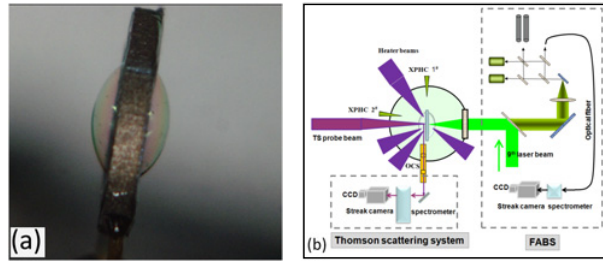


Figure 1. (a) The photograph of a typical gasbag target, (b) the setup of the experiment.

In this article, we present the investigation on the interaction of green laser pulse with millimeter-scale plasmas produced by gasbag target. Gasbag is suitable for the study of LPs due to its open geometrical structure that makes experimental setup more flexible [8, 9]. The plasmas are well characterized and the reflectivity of stimulated Raman scattering (SRS) and stimulated Brillouin scattering (SBS) is measured. The experimental results show that the reflectivity of SBS is less than 5% and that of SRS is less than 1% in our experimental condition. It is a positive result for using $0.53 \mu\text{m}$ laser as the driver for laser fusion.

2. EXPERIMENTAL SETUP

The gasbag target is fabricated by sticking two $0.4\text{-}\mu\text{m}$ -thick polyimide films to a $400\text{-}\mu\text{m}$ -thick Ti washer. The inner diameter of the washer is $1600 \mu\text{m}$. With the pressure of the filling gas through a thin tube mounted in the washer, the polyimide films expand and the overall diameter of the gasbag is approximately 1mm . Shown in Fig. 1(a) is the photograph of a typical gasbag target. The gasbag target is filled with neopentane (C_5H_{12}) with a pressure of 0.45 atm , that can lead to an electron density of about $4 \times 10^{20} \text{ cm}^{-3}$ with the assumption that the C_5H_{12} gas is fully ionized.

The experiments are performed on SG-II laser facility [10]. Shown in Fig. 1(b) is the schematic setup of the experiment. Four frequency-tripled (351 nm) heater beams are irradiated onto the target in the 60° cone. Each heater beam delivers an energy of 260 J within the duration of 1 ns . The diameter of the spot size of the heater beams on the gasbag films is about $400 \mu\text{m}$, leading to a nominal intensity of $2 \times 10^{14} \text{ W/cm}^2$. Two x-ray pinhole cameras (XPHCs) are used to monitor the time-integrated images of the plasmas: one for the side view and the other for the normal view. Both XPHCs are filtered with $200 \mu\text{m}$ Be film so that they can record the x rays above 2 keV .

The interaction beam can output 1 kJ within the duration of 1 ns at the wavelength of $0.53 \mu\text{m}$. It is focused to the center of the gasbag by an $f/5.4$ lens. A lens array is used for beam smoothing [11], resulting in a spot size of about $450 \times 450 \mu\text{m}^2$ and the nominal laser intensity is $5 \times 10^{14} \text{ W/cm}^2$. Both the TS probe beam and the interaction beam are delayed by 300 ps with respect to the four heater beams. A full-aperture backscattering system (FABS) is installed at the interaction beam. The FABS collects the back scattered light and provides the time-resolved and time-integrated reflectivity and the time-resolved spectrum of SRS and SBS. The temporal resolution of the system is about 100 ps .

A Thomson scattering (TS) system is set up to measure the electron temperature [12]. The TS probe beam can deliver 50 J energy at the wavelength of 263 nm within the duration of 1 ns . It is focused with an $f/12$ lens, leading to a spot size of about $100 \mu\text{m}$ in diameter. The scattered light is collimated and is focused into the entrance slit of a 750 mm spectrometer. The time-resolved spectrum is recorded with a streak camera. The scattering volume locates within the path of the interaction beam, and is about $100 \times 100 \times 130 \mu\text{m}^3$, which is determined by the spot size of the probe beam and the slit width of the spectrometer and the streak camera.

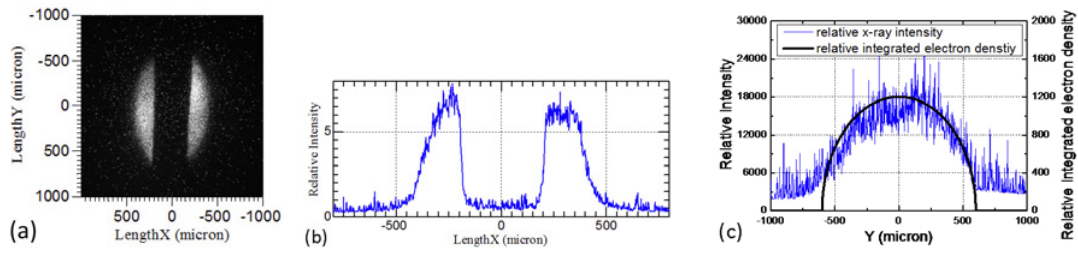


Figure 2. (a) Time-integrated x-ray image of a gasbag filled with CH, (b) the line profile along $Y = 0$, (c) the line profile along $X = 250 \mu\text{m}$.

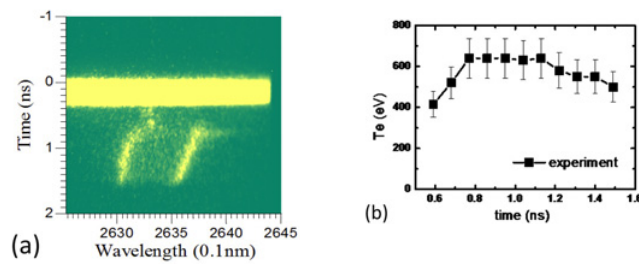


Figure 3. (a) A streaked Thomson scattering spectrum from CH-filled gasbag, (b) the inferred electron temperature versus time.

3. EXPERIMENTAL RESULTS AND DISCUSSIONS

Shown in Fig. 2(a) is the x-ray image of the gasbag from side view. The hemispherical image indicates that a millimeter-scale uniform plasmas is created. The line profile of the image along the horizontal line $Y = 0$ that passes through the center of the image is plotted in Fig. 2(b). The intensity distribution shows that the created plasma reached millimeter scale in horizontal direction. For detailed analysis, the vertical intensity distribution along $X = 250 \mu\text{m}$ is plotted in Fig. 2(c). The parabola-like intensity distribution is understandable for the gasbag target. The x rays detected by the XPHC are above 2 keV, which are optically thin. Thus the intensity of these x rays is proportional to the areal density of the plasma, i.e., the integrated electron density along the line of view. As seen in Fig. 2(c), the two profiles of the x-ray intensity and the integrated electron density agree well with each other, indicating sufficient heating of the gasbag.

Shown in Fig. 3 is the time-resolved TS spectrum of the CH-filled gasbag. The spectral separation between the two ion-acoustic peaks varies slowly during the laser pulse. Hence it is then inferred that the electron temperature of the CH plasmas remains constant. A two-ion-species theory for Thomson scattering [13] is applied to fit the TS spectrum and the inferred peak electron temperature is 640 eV. The obtained electron temperature versus time is presented in Fig. 3, showing that the electron temperature is nearly a constant between 0.7 ns and 1.3 ns.

In the experiment, the pressure of the filling gas C_5H_{12} is 0.45 atm, resulting in an electron density of $0.1 n_c$, where n_c is the critical density of the interaction beam. More accurate measurement of the electron density is obtained from the back SRS spectrum of the interaction beam. With the aid of the matching condition of SRS in combination with the dispersion relations of electron plasma waves and electromagnetic waves, the electron density can be inferred with the given electron temperature and the SRS wavelength. Shown in Fig. 4(a) is the streak image of the SRS spectrum from the CH gasbag. With the electron temperature obtained with TS, the inferred time-resolved electron density is shown in Fig. 4(b). We can see from Fig. 4(b) that the electron density remains at $0.1 n_c$ at early time ($t < 1.1 \text{ ns}$),

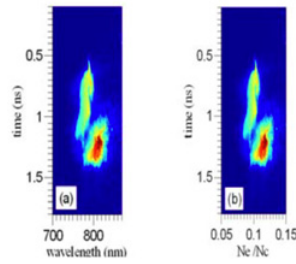


Figure 4. The streaked images of (a) SRS spectrum and (b) the corresponding electron density.

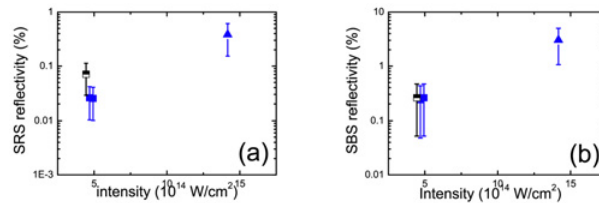


Figure 5. The reflectivity of (a) SRS and (b) SBS. The data in blue are obtained without the lens array.

consistent with that inferred from the pressure of the filling gas. At the time of 1.1 ns, the spectrum suffers a sudden wavelength shift toward longer wavelength corresponding to a higher electron density. This phenomenon can be ascribed to the propagation of the blast wave driven by the heater beams: when the blast-wave propagates into the resonance region of SRS, it causes a higher electron density and makes the SRS spectrum shift to longer wavelength.

The reflectivity of the SRS and SBS is measured with the FABS installed for the interaction beam. The integrated results in various conditions are shown in Fig. 5. We can see that both SRS and SBS are at a low level, with SRS below 1% and SBS below 5%. The reflectivity does not show significant enhancement even in high intensity ($1.5 \times 10^{15} \text{ W/cm}^2$) and no beam-smoothing condition. *The low reflectivity could partially be due to scattered light is out of the collection angle of the FABS. Another possible reason is the low electron temperature in the experiment: the electron plasma waves are heavily damped, and back scattered light is re-absorbed within the plasma.* Anyway, the low reflectivity of SRS and SBS indicates that it could be a promising way to achieve ignition by using $0.53 \mu\text{m}$ laser as the driver.

4. SUMMARY

In summary, millimeter-scale plasmas are successfully generated using a gasbag target on SG-II. Multiple diagnostics are applied to characterize the millimeter-scale plasmas. The images of the x-ray pinhole cameras confirm the plasma scale. The electron temperature, which remains stable near 640 eV, is diagnosed by a collective Thomson scattering system. The electron density is inferred through the back SRS spectrum, which is consistent with that inferred from the filling pressure of the gas. The reflectivity of SRS and SBS is rather low, indicating that green lasers could be suitable drivers for ICF.

This work is supported by the Natural Science Foundation of China (Grant Nos. 11005097, 11175179 and 236295), the Project of China Academy of Engineering Physics (Grant Nos. 9140C6801010901), and the Innovative Project of CAS (Grant No. KJCX2-YW-N36).

References

- [1] J. Lindl, *Phys. Plasmas* **2**, 3933 (1995)
- [2] S. H. Glenzer, B. J. MacGowan, and P. Michel et al., *Science* **327**, 1228 (2010)
- [3] W. L. Kruer, *The Physics of Laser Plasma Interactions* (Addison-Wesley, Redwood City 1988)
- [4] L. J. Suter, S. Glenzer, and S. Hann et al., *Phys. Plasmas* **11**, 2738 (2004)
- [5] C. Rousseaux, B. Meyer, and G. Thiell, *Phys. Plasmas* **2**, 2075 (1995)
- [6] R. M. Stevenson, K. Oades, and B. R. Thomas et al., *Phys. Rev. Lett.* **94**, 055006 (2005)
- [7] C. Niemann, R. L. Berger, and L. Divol et al., *Phys. Rev. Lett.* **100**, 045002 (2008)
- [8] D. H. Kalantar, D. E. Klem, and B. J. MacGowan et al., *Phys. Plasmas* **2**, 3161 (1995)
- [9] Z. C. Li, Q. Yin, and J. Zheng et al., *Chin. Phys. B* **19**, 125202 (2010)
- [10] Z. Lin, X. Deng, and D. Fan et al., *Fusion Eng. Des.* **44**, 66 (1999)
- [11] X. Deng, X. Liang, and Z. Chen et al., *Appl. Opt.* **25**, 377 (1986)
- [12] Z. B. Wang, J. Zheng, and B. Zhao et al., *Phys. Plasmas* **12**, 082703 (2005); Z. C. Li, J. Zheng, and X. H. Jiang et al., *Chinese Phys. Lett.* **28**, 125202 (2011)
- [13] D. E. Evans, *Plasma Phys.* **12**, 573 (1970)